Leucine-rich α2 -glycoprotein overexpression in the brain contributes to memory impairment

Chihiro Akiba [a], Madoka Nakajima [a], Masakazu Miyajima [a], Ikuko Ogino [a], Masami Miura [b], Ritsuko Inoue [b], Eri Nakamura [c], Fumio Kanai [c], Norihiro Tada [c], Miyuki Kunichika [d], Mitsutaka Yoshida [d], Kinya Nishimura [b,e], Akihide Kondo [a], Hidenori Sugano [a], Hajime Arai [a]

[a] Department of Neurosurgery, Juntendo University Graduate School of Medicine
2-1-1 Hongo Bunkyo-ku Tokyo 113-8421 JAPAN

[b] Neurophysiology Research Group, Tokyo Metropolitan Institute of Gerontology
35-2 Sakae-cho Itabashi-ku Tokyo 173-0015 JAPAN

[c] Laboratory of Disease Model Research, Juntendo University Graduate School of Medicine

[d] Laboratory of Morpheme Analysis Imaging Research, Juntendo University Graduate School of Medicine

[e] Department of Anesthesiology, Juntendo University Graduate School of Medicine

[c-e]: 2-1-1 Hongo Bunkyo-ku Tokyo 113-8421 JAPAN

Madoka Nakajima: madoka66@juntendo.ac.jp, Masakazu Miyajima: mmasaka@juntendo.ac.jp

Ikuko Ogino: i-ogino@juntendo.ac.jp, Masami Miura: mmiura@tmig.or.jp

Ritsuko Inoue: inoritu@centm.center.tmig.or.jp, Eri Nakamura: enakamur@juntendo.ac.jp

Fumio Kanai: fkanai@juntendo.ac.jp, Norihiro Tada: ntada@juntendo.ac.jp

Miyuki Kunichika: kunitika@juntendo.ac.jp, Mitsutaka Yoshida: myoshida@juntendo.ac.jp

Kinya Nishimura: juntendoski-50kinen@live.jp, Akihide Kondo: knd-aki@juntendo.ac.jp

Hidenori Sugano: debo@juntendo.ac.jp, Hajime Arai: harai@juntendo.ac.jp

*Correspondence to: Chihiro Akiba, Email: chihi-rocket@hotmail.co.jp

Abstract

We previously reported increase in leucine-rich α2-glycoprotein (LRG) concentration in cerebrospinal fluid is associated with cognitive decline in humans. To investigate relationship between LRG expression in the brain and memory impairment, we analyzed transgenic mice overexpressing LRG in the brain (LRG-Tg) focusing on hippocampus.

Immunostaining and western-blotting revealed age-related increase in LRG expression in hippocampal neurons in 8-, 24-, and 48-week-old controls and LRG-Tg. Y-maze and Morris water maze tests indicated retained spatial memory in 8- and 24-week-old LRG-Tg, while deteriorated in 48-week compared with age-matched controls. Field excitatory postsynaptic potentials declined with age in LRG-Tg compared with controls at 8-, 24- and 48-weeks. Paired-pulse ratio decreased with age in LRG-Tg, while increased in controls. As a result, long-term potentiation was retained in 8- and 24-week-old LRG-Tg, whereas diminished in 48-week-old compared with age-matched controls. Electron-microscopy observations

revealed fewer synaptic vesicles and junctions in LRG-Tg compared with age-matched controls, which became significant with age. Hippocampal LRG overexpression contributes to synaptic dysfunction, which leads to memory impairment with advance of age.

Keywords:

Leucine-rich α2-glycoprotein; Memory; Aging; Hippocampus; Synaptic plasticity; Field excitatory post-synaptic potentials; Long-term potentiation.

Abbreviations:

BBB: blood-brain barrier, LRG: leucine-rich α2-glycoprotein, LRR: leucine-rich repeats, CSF: cerebrospinal fluid, LRG-Tg: transgenic mice that conditionally overexpress LRG in the brain, GFAP: glial fibrillary acidic protein, mLRG: mouse LRG, hGFAP: human GFAP, PFA: paraformaldehyde, fEPSP: field excitatory post-synaptic potentials, PPR: paired-pulse ratio, LTP: long-term potentiation, PBS: phosphate buffered saline

1. Introduction

Cognitive decline is frequently associated with aging; however, the nature and severity of this decline vary considerably within a population. Thus, some clinical features are occasionally difficult to classify

55 into known dementia diseases such as Alzheimer's disease. In particular, mild cognitive dysfunction
56 appears similar to age-dependent physiological change. Aging demonstrably impairs episodic memory,
57 which is functionally linked to the hippocampus (Sama and Norris, 2013). Age-dependent blood-brain
58 barrier (BBB) breakdown in the human hippocampus has been reported (Montagne et al., 2015), and
59 chronic BBB breakdown is thought to lead to the accumulation of neurotoxic proteins causing progressive
60 neurodegeneration (Armulik et al., 2010, Toda, 2012). In the present study, the authors validated a protein
61 that increases in expression with aging and possibly exhibits neurotoxicity, which may be involved in
62 mild cognitive impairment.
63 Leucine-rich α2-glycoprotein (LRG), a 38- to 50- kDa glycoprotein containing leucine-rich repeats (LRR)
64 (Takahashi et al., 1985), was first identified in human serum in 1977 (Haupt and Baudner, 1977). The
65 LRR family of glycoproteins provides a versatile structural framework for protein-protein interactions
66 and serves multiple biological functions in vivo (Kobe and Kajava, 2001). LRG therefore is implicated
67 and increasingly expressed in a variety of physiological reactions, especially in inflammation-related
68 reactions such as early neutrophil granulocyte differentiation (O'Donnell et al., 2002), autoimmune
69 diseases (Serada et al., 2012, Ha et al., 2014), infectious diseases (Bini et al., 1996), and other
70 inflammatory diseases (Shirai et al., 2009, Chen et al., 2004), carcinogenesis and cancer progression
71 (Zhang et al., 2015, Takemoto et al., 2015), and pathogenic angiogenesis (Song and Wang, 2015, Wang et
72 al., 2013). Despite the wide array of functions that LRG performs, the pathological role of LRG in the

73 central nervous system has not been fully elucidated. LRG has been identified in both human cerebral
74 cortex (Nakajima et al., 2012, Miyajima et al., 2013) and cerebrospinal fluid (CSF; Li et al., 2006,
75 Nakajima et al., 2011). In a previous study, it was found that the LRG concentration in human CSF
76 increases with age, or due to neurodegenerative diseases such as Parkinson's disease with dementia,
77 dementia with Lewy bodies, and progressive supranuclear palsy (Miyajima et al., 2013). In addition,
78 increased LRG levels correlated with unfavorable Mini-Mental State Examination scores (Miyajima et al.,
79 2013), suggesting that LRG is implicated in age-related neurodegeneration.
80 The aim of the present study was to investigate the mechanism by which LRG impairs cognitive function.
81 To this end, a murine genetic construct that overexpresses LRG in the brain (LRG-Tg) was generated
82 (Miyajima et al., 2013), and consequent transgenic mice were analyzed especially for memory function
83 with a focus on the hippocampus, using behavioral tests, electrophysiological tests, and morphological
84 and histological analyses. 8-week-old mice were used as a young-age model, 24-week-old mice were
85 used as a middle age model, and 48-week-old mice were used as an old-age model. To our knowledge,
86 this is the first study to assess the relationship between LRG expression in the hippocampus and memory
87 function.
88

89 ## 2. Methods

90 ### 2.1. Animals

91 The generation of transgenic mice that conditionally overexpress LRG under a glial fibrillary acidic
92 protein (GFAP) promoter has been previously described (Miyajima et al., 2013). Briefly, mouse LRG
93 (mLRG) cDNA (BC030733, Thermo Fisher Scientific) was subcloned into a LoxP-GFP-pA-LoxP
94 construct that was excised with *Kpn*I and *Not*I. CAG-EGFP/mLRG^{LoxP} mice were crossed with human
95 GFAP (hGFAP)-Cre transgenic mice (B6.FVB-LRG-Tg [EIIa-Cre] C5379Lmgd/J; The Jackson
96 Laboratory) to produce a mouse with conditional Cre-mediated transgene expression
97 (CAG-EGFP/mLRGLoxP x hGFAP-Cre,). Transgenic mice lacking Cre recombinase were used as
98 controls.
99 All animal experiments were performed in accordance with the guidelines of the Laboratory Animal
100 Experimentation Committee of the Juntendo University School of Medicine, Japan, and approved by the
101 Institutional Animal Care and Use Committee of Juntendo University (Permit Number: 20-16). All
102 experimental mice were group-housed with 2 – 6 mice in a cage, and maintained in a
103 temperature-controlled and humidity-controlled facility (23 ± 1°C, 55 ± 5% humidity) on a 12-h
104 light/dark cycle. Mice that met the following criteria were excluded from the investigation: more than
105 20% weight loss, inability to walk/swim, LRG overexpression probed through western blotting in control
106 mice, and lowering LRG expression in LRG-Tg.
107 2.2. Observation of gross pathology and tissue preparation
108 Hippocampal weights and body weights were assessed for all age groups. Following body weight

measurement, mice were lethally anesthetized, subjected to cervical dislocation, decapitated, and rapidly harvested for whole brain tissues. The hippocampus was removed from one side, weighed, placed into an RNAlater® solution (QIAGEN), and stored at 4°C until use. The remaining side of the brain was stored in 10% paraformaldehyde (PFA) at 4°C until use.

2.3. Histopathological analysis

Sections stored in 10% PFA were cut into 4-μm-thick slices and incubated with primary antibody, rabbit anti-LRG138 (1:100 dilution; Immuno-Biological Laboratories) overnight at 4°C. Subsequently, sections were incubated with an appropriate secondary antibody (DAKO EnVision Labeled Polymer, Peroxidase; DAKO) for 30 min at 20°C. Reactions were detected using 0.05% 3,3′-diaminobenzidine tetrahydrochloride (DAB Tablet; Wako Pure Industries) as a chromogen and 0.05% hydrogen peroxide (H_2O_2) in phosphate-buffered saline (PBS). Sections were counterstained with Mayer's hematoxylin, dehydrated, mounted, and examined under a light microscope (E800; Nikon). Photomicrographs were acquired using a color digital camera affixed to the microscope (Axio Cam HRc; Carl Zeiss) using Axio Vision software (version 4.7; Carl Zeiss).

2.4. Western blotting analysis

Hippocampi stored in RNAlater® solution were homogenized in 200 μL of lysis buffer (N-PER; Thermo Fischer Scientific) containing protease inhibitor cocktail (cOmplete ULTRA Mini EDTA-free EASYpack; Roche). The lysates were clarified by centrifugation at 15,000 rpm for 10 min and the protein

127 concentrations of the resultant supernatants were determined using the BCA Protein Assay Kit (Thermo
128 Fischer Scientific). An equal amount of protein was then boiled for 5 min in EzApply loading buffer
129 (ATTO) containing 10 mM dithiothreitol. Samples were electrophoresed on an ePAGEL 10% sodium
130 dodecyl sulfate -polyacrylamide gel (ATTO) and subsequently transferred to a polyvinylidene difluoride
131 membrane (Thermo Fischer Scientific) using the iBlot Dry Blotting system (Thermo Fischer Scientific).
132 The primary antibody used was rabbit anti-LRG322 (1:100; Immuno-Biological Laboratories).
133 Membranes were operated using the WesternBreeze® Chromogenic Western Blot Immunodetection Kit
134 (Thermo Fischer Scientific) according to the manufacturer's specifications. Densitometry was performed
135 using ImageLab software (version 4.1; Bio-Rad Laboratories).
136 2.5. The Y-maze test
137 All behavioral experiments were performed by the same investigators, in the same laboratory, and at
138 approximately the same time every day, 10 a.m. to 1 p.m., during the light cycle.
139 First, spatial working memory was assessed using a Y-maze test (Chavant et al., 2010) with minor
140 modifications. Mice were placed at the end of one arm and allowed to move freely through the maze for 8
141 min. The total number of arm entries and alternations were recorded, wherein an entry was defined as
142 travel of at least 4 cm into a given arm, and alternation was defined as entry into each of the 3 arms
143 consecutively. Arm entries and path length were recorded by a computerized tracking system (Y-maze
144 Video Tracking System version 3; Muromachi Kikai). For analyses, the percent alternation was calculated

according to the following equation: percent alternation = (number of alternations)/(total number of arm entries - 2) × 100

2.6. The Morris water maze test

Three days after Y-maze testing, spatial learning and memory were assessed using a Morris water maze test (Morris et al., 1982) with minor modifications. The water was maintained at a temperature of 19 ± 2°C and rendered opaque by nontoxic white pigment. The pool was virtually divided into four quadrants of equal surface volume (Q1-4), and four different visual landmark cues were provided on the pool wall. During the learning trials, mice were trained to locate and climb a hidden platform that was submerged 0.5 cm below the water surface in the center of the north quadrant (Q1) of the pool. For each trial, the mouse was allowed 60 s to locate the platform; after locating and climbing the platform, the mouse was left on the platform for 10 s. If the mouse failed to locate the platform within 60 s, it was manually guided to the platform and left there for 10 s at the end of the trial. The latency to reach the platform and the swim path were recorded using a Morris Water Maze Video Tracking System (version 2.2; Muromachi Kikai). All mice were subjected to three training trials per day for 9 consecutive days. Approximately 24 h after the last training trial, a probe test was conducted. In the probe test, the platform was removed and each mouse was allowed to swim freely for 90 s. The time spent in Q1 and the swim path was recorded by the computerized tracking system (Morris Water Maze Video Tracking System version 2.2).

2.7. Electrophysiological phenotyping

163 Evoked field excitatory post-synaptic potentials (fEPSPs) were recorded in the hippocampal slices
164 obtained from controls and LRG-Tg. Hippocampal slices (300 μm) were prepared as previously described
165 (Miura et al., 2002).
166 The fEPSPs were recorded using a borosilicate glass pipette filled with artificial CSF composed of (in
167 mM) the following: 124 NaCl, 26 $NaHCO_3$, 10 glucose, 1 NaH_2PO_4, 3 KCl, 1.2 $MgCl_2$, and 2.4 $CaCl_2$,
168 bubbled with 95% O_2 and 5% CO_2, pH 7.4. The recording pipette was placed in the stratum radiatum of
169 CA1. The fEPSPs were evoked by stimulating the Schaffer collateral/commissural pathway, wherein a
170 glass stimulating electrode filled with 1M NaCl (resistance < 1 MΩ) was placed at a distance of 400 μm
171 from the recording electrode. Signals were sampled at 20 kHz and filtered at 2 kHz using an Axoclamp
172 2B amplifier (Molecular Devices), digitized with an ITC-16 data acquisition interface (HEKA Electronik;
173 formerly Instrutech), and analyzed with Pulse 8.80 software (HEKA Elektronik). The stimulation strength
174 was adjusted to 25–40% of the maximal fEPSP slope. In all experiments, baseline fEPSPs were evoked
175 with short pulses (100 μs at 0.067 Hz) and recorded for at least 20 min. The paired-pulse ratio (PPR) was
176 calculated as the quotient of fEPSPs (second slope/first slope) recorded during the paired stimulation in
177 20- to 500-ms intervals.
178 Long-term potentiation (LTP) was induced with high-frequency stimulation consisting of 30-100 pulses at
179 100 Hz (baseline stimulation strength) and its magnitude was measured over a 60- min period. The
180 formation of late-phase LTP is known to require strong stimulation (e.g., repeated tetanic stimuli) (Huang

and Kandel, 1994, Sajikumar et al., 2008). Therefore, three trains of high-frequency stimulation were applied (100 pulses at 100 Hz) at 15 s intervals, and the magnitude of the LTP was measured for 4 h. Late-phase LTP analyses were conducted in hippocampal slices of 24-week-old mice. The magnitude of LTP was expressed as the fEPSP slope normalized to the average slope of baseline recordings.

2.8. Electron microscopy observation

Mice were perfused with 4% PFA containing 2.5% glutaraldehyde in PBS (pH 7.4). Fixed cerebral samples were dissected out, sectioned into small pieces (3×3 mm, 1–2 mm thick), and post-fixed overnight in PBS containing 2.5% glutaraldehyde at 4°C. Ultrathin sections were observed under an HT7700 electron microscope (Hitachi High-Technologies). The numbers of synaptic vesicles and synaptic junctions per unit area (58.3 μm^2 at 5000×) were counted in 10 randomly selected visual fields from within the CA1 hippocampal region.

2.9. Statistics

All analyses were performed using SPSS version 18 (IBM). Statistical analyses were designed using the assumption of normal distribution and similar variance among groups. To assess between-group differences with regard to band intensities of western blot analyses, weight measurements, behavioral assay variables, and electrophysiological studies, two-tailed Student's *t*-tests were used.

2.10. Experimental design

The exact number of experimental animals for each experiment is described in Supplementary Data 5. To

199 decide the sample number, we planned a study of independent cases and controls with 1 control per case.
200 Prior data indicated that the probability of exposure among controls is 0.1. In case the true probability of
201 exposure among cases is 0.6, we needed to study 13 LRG-Tg and 13 control mice. This would allow us to
202 reject the null hypothesis that the exposure rates for case and controls are equal with a probability (power)
203 of 0.8. The type I error probability associated with this test of the null hypothesis was 0.05. We used an
204 uncorrected χ^2 statistic to evaluate the null hypothesis. A discrepancy between the number of mice in the
205 plan and in the actual study came from the difference in the number of mice born between the control and
206 LRG-Tg. No randomization or blinding was used in this study. As the behavioral tests were recorded
207 using a video tracking system as described above, knowing the group allocation would not have
208 influenced the results.
209

210 3. Results

211 3.1. LRG expression increases with age in the murine hippocampus

212 LRG immunoreactivity was predominantly observed in the cytoplasm of neurons in the CA3 hippocampal
213 region, and to a lesser extent, in the CA1 region (Fig. 1A). Immunohistochemical and western blot
214 analyses showed LRG immunoreactivity increases with age in control mice ($p = 0.047$ to < 0.001). It is
215 understandably that LRG expression was found to be greater in LRG-Tg than in age-matched control
216 mice ($p < 0.001$, Fig. 1A, B, C). Data regarding specific band intensities are provided in Supplementary

217 Data 3D.

218 3.2. Hippocampal volume is reduced in LRG-Tg

219 Hippocampal weights were significantly reduced in LRG-Tg compared with control mice in all age

220 groups ($p < 0.001$, Fig. 1D, Supplementary Data 3A). On the other hand, control and LRG-Tg body

221 weights were similar ($p = 0.055$-0.532, Supplementary Data 1A, 3F), and no gross neuroanatomical

222 anomaly was detected in LRG-Tg (Supplementary Data 1B).

223 3.3. Spatial memory is impaired in old LRG-Tg

224 In the Y-maze test, percent alternation was not different between control mice and LRG-Tg at 8 and 24

225 weeks of age ($p = 0.774$ and 0.329, respectively), whereas that at 48 weeks of age was significantly lower

226 in LRG-Tg than in controls ($p = 0.017$, Fig. 2A), suggesting that immediate spatial short-term memory

227 was exclusively impaired in 48-week-old LRG-Tg. To confirm that the group differences in alternation

228 were not due to variations in motor function or motivation, walking speed was measured in each group

229 and no significant differences were observed ($p = 0.104$, 0.399, and 0.312, Supplementary Data 2A).

230 In the Morris water maze test, representative pathways recorded from 48-week-old mice during the

231 learning period are shown in Fig. 2B, which summarizes our findings showing rapid shortening of path

232 length to reach the platform in control mice, which is less apparent in LRG-Tg. Similarly, no significant

233 between-group differences were detected in terms of latency to reach the hidden platform in mice aged 8-

234 and 24-weeks during the learning period ($p = 0.101$-0.932 and $p = 0.090$-0.924, respectively, Fig. 2C).

235 Similarly, in 48-week-old mice, no significant between-group differences were observed in the first 2
236 days of the learning period (p = 0.066 and 0.287). However, from day 3, LRG-Tg aged 48 weeks
237 exhibited longer latencies to reach the platform than control mice (p = 0.006-0.046, Fig. 2D), suggesting
238 an impairment of spatial learning in 48-week-old LRG-Tg. In the probe test, when the platform was
239 removed from the original position (Q1), the percentage of time spent in Q1 within 90 s (i.e., the entire
240 testing time) is indicated as time in Q1 (%). The time in Q1 (%) was not different between groups at 8
241 and 24 weeks (p = 0.691 and 0.434, respectively), suggesting retention of spatial learning memory formed
242 in the learning period. However, at 48 weeks of age, time in Q1 (%) was significantly lower in LRG-Tg
243 than in controls (p = 0.046, Fig. 2E, F). To confirm that group differences in escape latency were not
244 linked to variations in swimming ability or motivation, swimming speed (cm/s) was measured in each
245 group during the learning period (p = 0.063-0.963, Supplementary Data 2B) and the probe test (p = 0.318,
246 0.395, and 0.238, Supplementary Data 2C); no significant differences were observed between groups. The
247 complete dataset for the behavioral tests is provided in Supplementary Data 3B.
248 3.4. Synaptic transmission and synaptic plasticity are impaired in old LRG-Tg
249 Electrophysiological characterization was used to analyze possible mechanisms of memory impairment in
250 48-week-old LRG-Tg. The fEPSPs were significantly smaller in LRG-Tg than in controls at all ages
251 examined ($p < 0.05$, $p < 0.01$, and $p < 0.01$), indicating an impairment of synaptic transmission in
252 LRG-Tg, and these differences became evident with age (Fig. 3A). Next, the PPRs of fEPSP slopes

253 (second slope/first slope) following paired stimulation at intervals of 25-500 ms were calculated. At 8
254 weeks of age, PPR values were larger in hippocampal slices obtained from LRG-Tg than in those
255 obtained from control mice. However, PPR values increased with age in control mice, whereas those of
256 LRG-Tg decreased. Therefore, the PPR trends were ultimately reversed at 48-weeks of age in control and
257 LRG-Tg (Fig. 3B).
258 To investigate the effects of LRG overexpression on synaptic plasticity, we next evaluated LTP induced
259 by high-frequency stimulation (100 pulses at 100 Hz) of Schaffer-collaterals. The magnitude of LTP
260 remained stable at 60 min post-stimulation in 8- and 24-week-old LRG-Tg relative to age-matched
261 controls ($p = 0.698$ and 0.130, respectively). In contrast, LTP was significantly diminished 60 min after
262 high-frequency stimulation in 48-week-old LRG-Tg compared with that of age-matched control mice,
263 suggesting the attenuation of synaptic plasticity ($p = 0.014$, Fig. 3C). Regarding LTP phenotyping of
264 8-week-old, 24-week-old LRG-Tg showed a certain difference compared with age-matched controls,
265 which, however, was not statistically significant. Thus, we used short tetanic stimulation (30 pulses at 100
266 Hz) to examine the subtle differences between controls and LRG-Tg in LTP threshold in 24-week-old
267 mice. As a result, a significantly smaller magnitude of LTP was induced in 24-week-old LRG-Tg relative
268 to that in age-matched controls ($p = 0.047$, Fig. 3D), suggesting that the LRG-Tg feature an increased
269 threshold for LTP formation relative to control mice. Comparatively, no between-group difference was
270 observed in the 4 h stability of late-phase LTP induced by three trains of high-frequency stimulation in

24-week-old mice (p = 0.324, Fig. 3E). The complete electrophysiological dataset is found in Supplementary Data 3C.

3.5. Synaptic formation is impaired in LRG-Tg

Electron microscopy of the CA1 hippocampal region in 10 visual fields at 5000× magnification revealed the numbers of synaptic junctions and synaptic vesicles present in the region (Fig. 4A-C). Significant differences were observed between controls and LRG-Tg, which became obvious with aging (p =0.025 to < 0.001, Fig. 4D, E). The electron microscopy data are provided in Supplementary Data 3E.

4. Discussion

In the present study, we focused on the hippocampus of LRG-Tg which overexpress LRG in the brain, to analyze the effect of LRG on memory function. Age-related accumulation of LRG was observed in hippocampal neurons, in both controls and LRG-Tg. Spatial memory formation was retained in control mice, even at 48 weeks of age. However, memory function was significantly impaired in 48-week-old LRG-Tg, in contrast to retention in 24-week-old LRG-Tg. These findings suggest that memory function is impaired due to abnormal LRG overexpression, and not due to the regulated amount of LRG accumulation as a part of the normal aging process.

LTP induced by high-frequency stimulation (100 pulses at 100 Hz) of Schaffer collaterals was significantly diminished in 48-week-old LRG-Tg relative to that of age-matched controls at 60 min after

289 stimulation, whereas LTP remained stable in 8- and 24-week-old LRG-Tg. This result indicates that
290 memory formation is impaired in 48-week-old mice only under the condition of LRG overexpression.
291 Focusing on the subtle decline in 24-week-old LRG-Tg in LTP induced by high-frequency stimulation,
292 LTP induced by short tetanic stimulation was used to investigate the threshold of LTP formation.
293 Consequently, an increased threshold was identified in LRG-Tg compared with age-matched control mice.
294 On the other hand, the 24-week-old LRG-Tg phenotype had no effect on the induction or stability of
295 late-phase LTP induced by three trains of high-frequency stimulation. These data suggest that synaptic
296 plasticity is impaired in LRG-Tg in response to weak stimulation, but not in response to strong
297 stimulation, indicating mild memory dysfunction with the possibility of catching up under conditions of
298 strong or repeated stimulation. Since LTP is considered to reflect the synaptic basis of learning and
299 memory in hippocampal neurons (Bliss and Collingridge, 1992), such findings are consistent with the
300 results of the probe test conducted in Morris water maze testing, in which 48-week-old LRG-Tg showed
301 impaired spatial memory, while 24-week-old LRG-Tg retained spatial memory.
302 Synaptic dysfunction was indicated in LRG-Tg at all ages, as evidenced by the depression of fEPSP
303 slopes, which represent changes in the electrical potential of the post-synaptic junction. Notably, the
304 depression became more severe with aging. However, the PPR values of controls and LRG-Tg showed an
305 opposing tendency, when compared at 48 and 8 weeks of age. Previous studies have noted that an
306 increased PPR value represents a decreased release probability in pre-synaptic terminals (Heinl et al.,

307 2011). Thus, interestingly, the phenotype of PPR in LRG-Tg indicated that transmission efficiency
308 increased with age, whereas the reverse was observed in control mice. This phenomenon might be
309 explained as a pre-synaptic compensatory change following the severe synaptic dysfunction that worsens
310 with age in LRG-Tg. Therefore, the electrophysiological phenotypes indicated LTP impairment in
311 48-week-old LRG-Tg, which was suggested to be based on an increased threshold required for LTP
312 formation. The fact that LTP induced by high-frequency stimulation was retained in 24-week-old LRG-Tg
313 despite the fEPSP decline could be explained by a decreased PPR, indicating a compensatory increase of
314 transmission efficiency in the pre-synaptic system.
315 As a conclusion of the present study, LRG overexpression in hippocampal neurons contributes to memory
316 impairment in age-advanced mice. It is related to the suppression of LTP formation attributed to
317 age-related synaptic dysfunction indicated by the fEPSP decline and compensatory reaction suggested by
318 the decreased PPR.
319 Numerous studies have reported a relationship between the inflammatory response and neurodegeneration,
320 including increased expression of cytokines, complement proteins, degradative enzymes, and adhesion
321 molecules and increased production of reactive oxygen species along with prominent cellular activation
322 of microglia and astrocytes (Lynch, 2014, Rampa et al., 2013, Lane et al., 2012, Sastre et al., 2011).
323 Moreover, chronic systemic inflammation (Liu et al., 2012), as well as neuro-inflammation (Di Filippo et
324 al., 2013, Griffin et al., 2006, O'Donnell et al., 2000, Murray and Lynch, 1998), is thought to be

325 responsible for the age-related LTP impairment. In the present study, we have shown that the mechanism
326 of memory impairment as a result of LRG overexpression. Since LRG expression is reported to increase
327 under the condition of chronic inflammation in humans, as described in the Introduction, and moreover, is
328 considered to be induced by inflammatory cytokines (Fujimoto et al., 2015), anti-inflammatory measures
329 have therapeutic potential for suppression of LRG accumulation leading to the preservation of cognitive
330 function. For instance, lenalidomide, an inhibitor of tumor necrosis factor-α, suppresses LRG secretion in
331 the bone marrow of osteoarthritis joints (Wang et al., 2017), and tocilizumab, an anti-interleukin-6
332 receptor antibody, reduces serum LRG levels in patients with rheumatoid arthritis. Additionally, although
333 not specific to LRG, non-steroidal anti-inflammatory drugs (Etminan et al., 2003, Kotilinek et al., 2008),
334 control of diabetes (Kawamura et al., 2012), manipulation of suppressor of cytokine signaling protein
335 expression (Walker et al., 2015), long chain omega-3 fatty acids (Thomas et al., 2015), and prazosin, an
336 α_1-adrenoceptor antagonist (Katsouri et al., 2013), are all reported to be involved in the mechanisms of
337 anti-inflammatory effects leading to the suppression of neurodegeneration progression. Elucidating the
338 relationship between anti-inflammation therapy and LRG suppression in the brain will constitute the
339 research task now and in the future.
340

341 ## Conclusion

342 We posit LRG overexpression in hippocampal neurons as a precipitating factor for memory dysfunction

in later life. Age-related synaptic dysfunction and compensatory change play important roles in LRG-overexpression-related memory dysfunction.

Acknowledgements

The authors would like to thank Katsumi Miyahara and Yasuko Toi (Laboratory of Morpheme Analysis Imaging Research, Juntendo University Graduate School of Medicine) for their guidance in preparing frozen samples and the use of their experimental facilities, Mika Kikkawa (Laboratory of Biomolecule Research, Juntendo University Graduate School of Medicine) for supervision in bioinformatics analysis, Jin Takahashi (Muromachi Kikai) for providing support during behavioral tests, Ivana Jurjevic (Department of Pharmacology and Department of Neurology, University of Zagreb), Kostadin L. Karagiozov (Department of Neurosurgery, Juntendo University Graduate School of Medicine), and Elsevier's English Language Editing service for English language editing.

This work was supported by JSPS KAKENHI Grant Number B#26293326 and C#26462217 from the Japan Society for the Promotion of Science, a Grant-in-Aid for Encouragement of Scientists from Juntendo University Research Institute for Diseases of Old Age (Tokyo, Japan), and a Grant-in-Aid for Encouragement of Scientists from Juntendo University Graduate School of Medicine (Tokyo, Japan).

Disclosure statement

361 The authors declare that they have no competing financial interests.

362

363 ## References

364 Armulik A, Genove G, Mae M, Nisancioglu MH, Wallgard E, Niaudet C, He L, Norlin J, Lindblom

365 P, Strittmatter K, Johansson BR, Betsholtz C. Pericytes regulate the blood–brain barrier. Nature

366 2010; 468, 557-62.

367 Bini L, Magi B, Marzocchi B, Cellesi C, Berti B, Raggiaschi R, Rossolini A, Pallini V.

368 Two-dimensional electrophoretic patterns of acute-phase human serum proteins in the course of

369 bacterial and viral diseases. Electrophoresis 1996; 17: 612-6.

370 Bliss TVP, Collingridge GL. A synaptic model of memory: long-term potentiation in the

371 hippocampus. Nature 1992; 361: 31-9.

372 Chavant F, Deguil J, Pain S, Ingrand I, Milin S, Fauconneau B, Perault-Pochat MC,

373 Lafay-Chebassier C. Imipramine, in part through tumor necrosis factor α inhibition, prevents

374 cognitive decline and β-amyloid accumulation in a mouse model of Alzheimer's disease. J.

375 Pharmacol. Exp. Ther. 2010; 332: 505-14.

376 Chen JH, Chang YW, Yao CW, Chiueh TS, Huang SC, Chien KY, Chen A,

377 Chang FY, Wong CH, Chen YJ. Plasma proteome of severe acute respiratory syndrome

378 analyzed by two-dimensional gel electrophoresis and mass spectrometry. Proc. Natl. Acad. Sci.

U. S. A. 2004; 101: 17039–44.

Di Filippo M, Chiasserini D, Gardoni F, Viviani B, Tozzi A, Giampa C, Costa C, Tantucci M, Zianni E, Boraso M, Siliquini S, de Iure A, Ghiglieri V, Colcelli E, Baker D, Sarchielli P, Fusco FR, Di Luca M, Calabresi P. Effects of central and peripheral inflammation on hippocampal synaptic plasticity. Neurobiol Dis. 2013; 52: 229-236.

Etminan M, Gill S, Samii A. Effect of non-steroidal anti-inflammatory drugs on risk of Alzheimer's disease: systematic review and meta-analysis of observational studies. BioMed Journal 2003; 327: 128.

Fujimoto M, Serada S, Suzuki K, Nishikawa A, Ogata A, Nanki T, Hattori K, Kohsaka H, Miyasaka N, Takeuchi T, Naka T. Leucine-rich α_2-glycoprotein as a potential biomarker for joint inflammation during anti-interleukin-6 biologic therapy in rheumatoid arthritis. Arthritis Rheumatol. 2015; 67 (8): 2056-2060.

Griffin R, Nally R, Nolan Y, McCartney Y, Linden J, Lynch MA. The age-related attenuation in long-term potentiation is associated with microglial activation. J Neurochem. 2006; 99: 1263-1272.

Ha YJ, Kang EJ, Lee SW, Lee SK, Park YB, Song JS, Choi ST. Usefulness of serum leucine-rich alpha-2 glycoprotein as a disease activity biomarker in patients with rheumatoid arthritis. J Korean Med Sci 2014; 29: 1199-204.

Haupt H, Baudner S. Isolation and characterization of an unknown, leucine-rich 3.1-S-alpha2-glycoprotein from human serum (author's translation). Hoppe-Seyler's Z. Physiol.Chem 1977; 358: 639-46.

Heinl C, Drdla-Schutting R, Xanthos DN, Sandkuhler J. Distinct mechanisms underlying pronociceptive effects of opioids. J. Neurosci. 2011; 31: 16748–56.

Huang YY, Kandel ER. Recruitment of long-lasting and protein kinase A-dependent long-term potentiation in the CA I region of hippocampus requires repeated tetanization. Learn. Mem. 1994; 1: 74-82.

Kawamura A, Umemura T, Hotta N. Cognitive impairment in diabetic patients: Can diabetic control prevent cognitive decline? J Diabetes Invest 2012; 3**:** 413-23.

Kobe B, Kajava A. The leucine-rich repeat as a protein recognition motif. Curr. Opin. Struct. Biol. 2001; 11: 725–32.

Katsouri L, Vizcaychipi MP, McArthur S, Harrison I, Suarez-Calvet M, Lleo A, Lloyd DG, Ma D, Sastre M. Prazosin, an α1-adrenoceptor antagonist, prevents memory deterioration in the APP23 transgenic mouse model of Alzheimer's disease. Neurobiol. Aging 2013; 34: 1105-15.

Kotilinek LA, Westerman MA, Wang Q, Panizzon K, Lim GP, Simonyi A, Lesne S, Falinska A, Younkin LH, Younkin SG, Rowan M, Cleary J, Wallis RA, Sun GY, Cole G, Frautschy S, Anwyl R, Ashe KH. Cyclooxygenase-2 inhibition improves amyloid-beta-mediated suppression of

415 memory and synaptic plasticity. Brain 2008; 131: 651-64.

416 Lane RF, Shineman DW, Steel JW, Lee LB, Fillit HM. Beyond amyloid: the future of therapeutics

417 for Alzheimer's disease. Adv Pharmacol. 2012; 64: 213–71.

418 Li X, Miyajima M, Mineki R, Taka H, Murayama K, Arai H. Analysis of potential diagnostic

419 biomarker in cerebrospinal fluid of idiopathic normal pressure hydrocephalus by proteomics.

420 Acta Neurochir (Wien) 2006; 148: 859-64.

421 Liu X, Wu Z, Hayashi Y, Nakanishi H. Age-dependent neuroinflammatory responses and deficits in

422 long-term potentiation in the hippocampus during systemic inflammation. Neuroscience 2102;

423 216: 133-142

424 Lynch MA. The impact of neuroimmune changes on development of amyloid pathology; relevance

425 to Alzheimer's disease. Immunology 2014; 141: 292–301.

426 Murray CA, Lynch MA. Evidence that increased hippocampal expression of the cytokine

427 interleukin-1β is a common trigger for age- and stress-induced impairment in long-term

428 potentiation. J Neurosci. 1998; 18: 2974-2981.

429 Miura M, Watanabe M, Offermanns S, Simon MI, Kano M. Group I metabotropic glutamate

430 receptor signaling via Gq/G11 secures the induction of long-term potentiation in the

431 hippocampal area CA1. J. Neurosci. 2002; 22: 8379–90.

432 Miyajima M, Nakajima M, Motoi Y, Moriya M, Sugano H, Ogino I, Nakamura E, Tada N,

433 Kunichika M, Arai H. Leucine-rich α2-glycoprotein is a novel biomarker of neurodegenerative
434 disease in human cerebrospinal fluid and causes neurodegeneration in mouse cerebral cortex.
435 PLoS One 2013; 8: e74453.
436 Montagne A, Barnes SR, Sweeney MD, Halliday MR, Sagare AP, Zhao Z, Toga AW, Jacobs RE,
437 Liu CY, Amezcua L, Harrington MG, Chui HC, Law M, Zlokovic BV. Blood-brain barrier
438 breakdown in the aging human. Neuron 2015; 85: 296–302.
439 Morris RGM, Garrud JNP, Rawlins JNP, O'Keefe J. Place navigation impaired in rats with
440 hippocampal lesions. Nature 1982; 297: 681-3.
441 Nakajima M, Miyajima M, Ogino I, Watanabe M, Miyata H, Karagiozov KL, Arai H, Hagiwara Y,
442 Segawa T, Kobayashi K, Hashimoto Y. Leucine-rich α2-glycoprotein is a marker for idiopathic
443 normal pressure hydrocephalus. Acta Neurochir (Wien) 2011; 153:1339-46.
444 Nakajima M, Miyajima M, Ogino I, Watanabe M, Hagiwara Y, Segawa T, Kobayashi K, Arai H.
445 Brain localization of leucine-rich α2-glycoprotein and its role. Acta Neurochirur. Suppl. 2012;
446 113: 97-101.
447 O'Donnell E, Vereker E, Lynch MA. Age-related impairment in LTP is accompanied by enhanced
448 activity of stress-activated protein kinases: analysis of underlying mechanism. Eur J Neurosci.
449 2000; 12: 345-352.
450 O'Donnell LC, Druhan LJ, Avalos BR. Molecular characterization and expression analysis of

leucine-rich α2-glycoprotein, a novel marker of granulocytic differentiation. J. Leukoc. Biol. 2002; 72: 478–85.

Rampa A, Gobbi S, Belluti F, Bisi A. Emerging targets in neurodegeneration: new opportunities for Alzheimer's disease treatment? Curr Top Med Chem. 2013; 13: 1879–904.

Sajikumar S, Navakkode S, Frey JU. Distinct single but not necessarily repeated tetanization is required to induce hippocampal late-LTP in the rat CA1. Learn. Mem. 2008; 15: 46-9.

Sama DM, Norris CM. Calcium dysregulation and neuroinflammation: Discrete and integrated mechanisms for age-related synaptic dysfunction. Ageing Res Rev 2013; 12: 982-95.

Sastre M, Richardson JC, Gentleman SM, Brooks DJ. Inflammatory risk factors and pathologies associated with Alzheimer's disease. Curr Alzheimer Res. 2011; 8: 132–41.

Serada S, Fujimoto M, Terabe F, Iijima H, Shinzaki S, Matsuzaki S, Ohkawara T, Nezu R, Nakajima S, Kobayashi T, Plevy SE, Takehara T, Naka T. Serum leucine-rich alpha-2 glycoprotein is a disease activity biomarker in ulcerative colitis. Inflamm. Bowel Dis. 2012; 18: 2169-79.

Shirai R, Hirano F, Ohkura N, Ikeda K, Inoue S. Up-regulation of the expression of leucine-rich α2-glycoprotein in hepatocytes by the mediators of acute-phase response. Biochem. Biophys. Res. Commun. 2009; 382: 776-9.

Song W, Wang X. The role of TGFβ1 and LRG1 in cardiac remodeling and heart failure. Biophys. Rev. 2015; **7**: 91–104.

469 Takahashi N, Takahashi Y, Putnam FW. Periodicity of leucine and tandem repetition of a 24-amino
470 acid segment in the primary structure of leucine-rich α2-glycoprotein of human serum. Proc. Nat.
471 Acad. Sci. U. S. A. 1985; 82: 1906-10.
472 Takemoto N, Serada S, Fujimoto M, Honda H, Ohkawara T, Takahashi T, Nomura S, Inohara H,
473 Naka T. Leucine-rich α-2-glycoprotein promotes TGFβ1-mediated growth suppression in the
474 Lewis lung carcinoma cell lines. Oncotarget 2015; 10: 11009-22.
475 Thomas J, Thomas CJ, Radcliffe J, Itsiopoulos C. Omega-3 fatty acids in early prevention of
476 inflammatory neurodegenerative disease: A focus on Alzheimer's disease. BioMed Research
477 International 2015; doi:10.1155/2015/17280.
478 Toda N. Age-related changes in endothelial function and blood flow regulation. Pharmacol Ther
479 2012; 133: 159-76.
480 Walker DG, Whetzel AM, Lue LF. Expression of suppressor of cytokine signaling (SOCS) genes in
481 human elderly and Alzheimer's disease brains and human microglia. Neuroscience. 2015; 302:
482 121–37.
483 Wang X, Abraham S, McKenzie JAG, Jeffs N, Swire M, Tripathi VB, Luhmann UFO, Lange CAK,
484 Zhai Z, Arthur HM, Bainbridge J, Moss SE, Greenwood J. LRG1 promotes angiogenesis by
485 modulating endothelial TGFß signaling. Nature 2013; 499: 306-11.
486 Wang Y, Xu J, Zhang X, Wang C, Huang Y, Dai K, Zhang X. TNF-α-induced LRG1 promotes

angiogenesis and mesenchymal stem cell migration in the subchondral bone during osteoarthritis. Cell Death Dis. 2017; 8, e2715.

Zhang Y, Luo Q, Wang N, Hu F, Jin H, Ge T, Wang C, Qin W. LRG1 suppresses the migration and invasion of hepatocellular carcinoma cells. Med. Oncol. 2015; 32.

Figures and figure legends

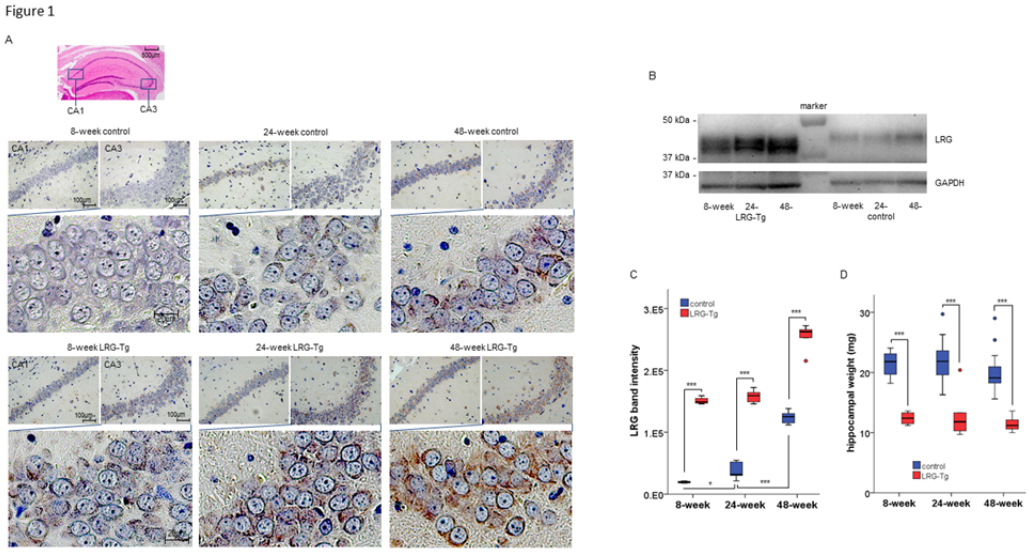

Figure 1. Histopathological findings in the hippocampus. (**A**) LRG immunoreactivity in the neuronal cytoplasm in the CA1 and CA3 hippocampal region indicates age-dependent accumulation of LRG in control mice. LRG expression was higher in LRG-Tg than in age-matched control mice. (**B**) Representative cropped image of western blotting for LRG in 8-week-old control (n = 4) and LRG-Tg (n = 4), 24-week-old control (n = 5) and LRG-Tg (n = 7), and 48-week-old control (n = 7) and LRG-Tg (n = 5) mice. (**C**) Quantification of the corresponding band intensities produced results similar to those

obtained from the immunohistochemical analysis. (**D**) The hippocampal weights measured in 8-week-old control (n = 8) and LRG-Tg (n = 8), 24-week-old control (n = 19) and LRG-Tg (n = 14), and 48-week-old control (n = 19) and LRG-Tg (n = 13) mice were lower in LRG-Tg than in control mice at all ages examined.

All images displayed are representative and values are expressed as the median (interquartile range 25% and 75%) of independent experimental groups. To assess between-group differences, 2-tailed Student's *t*-tests were used. ***$p < 0.001$.

Figure 2

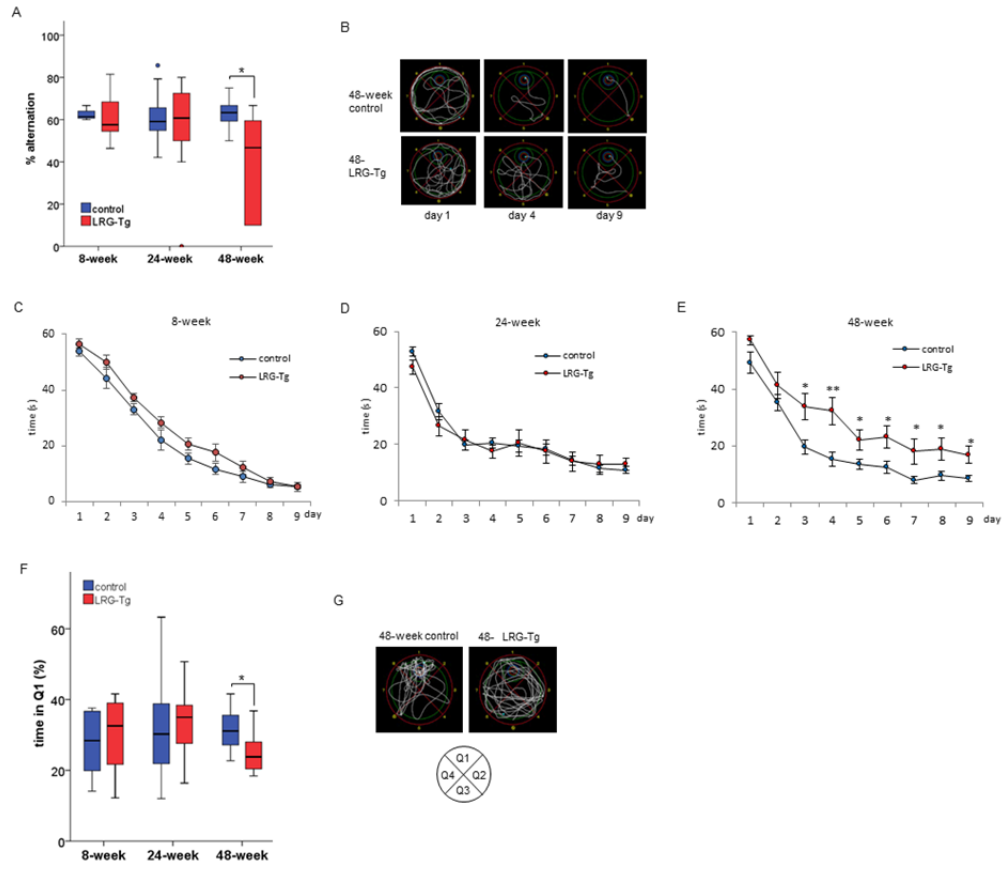

Figure 2. The findings in spatial memory testing. (**A**) The percentage alternation in the Y-maze test was

significantly lower in 48-week-old LRG-Tg compared with age-matched control mice, but not significantly different in 24-week-old mice: 8-week-old control (n = 6) and LRG-Tg (n = 11), 24-week-old control (n = 47) and LRG-Tg (n = 18), and 48-week-old control (n = 17) and LRG-Tg (n = 19). (**B**) The representative pathway recorded for 48-week-old mice during learning periods. The pathway observed in control mice rapidly shortened during the period, while that of LRG-Tg showed slower shortening. (**C**, **D**, **E**) The latency to reach the hidden platform in the probe test of Morris water maze testing; no significant differences were observed in 8-week-old (n = 6 controls and 6 LRG-Tg) and 24-week-old mice (n = 36 controls and 16 LRG-Tg 16) during the period, while 48-week-old LRG-Tg (n = 13 control 13 and 9 LRG-Tg) displayed longer latencies than age-matched controls from day 3. (**F**) The percentage of time spent in Q1 during the entire testing time (i.e., 90 s), is indicated as 'time in Q1 (%)'. In the probe test, time in Q1 (%) obtained from 8-week-old (n = 6 controls and 6 LRG-Tg) and 24-week-old controls and LRG-Tg (n = 38 controls and 22 LRG-Tg) were not significantly different. However, time in Q1 (%) was significantly lower in 48-week-old LRG-Tg than in age-matched controls (n = 19 controls and 9 LRG-Tg). (**G**) The pathway recorded for 48-week-old mice during the probe test. All images displayed are representative and values are expressed as the median (interquartile range 25% and 75%) for (A) and (E) and the mean ± S.E.M. for (C) and (D) of independent experimental groups. To assess between-group differences, 2-tailed Student's *t*-tests were used.* $p < 0.05$; **$p < 0.01$.

Figure 3

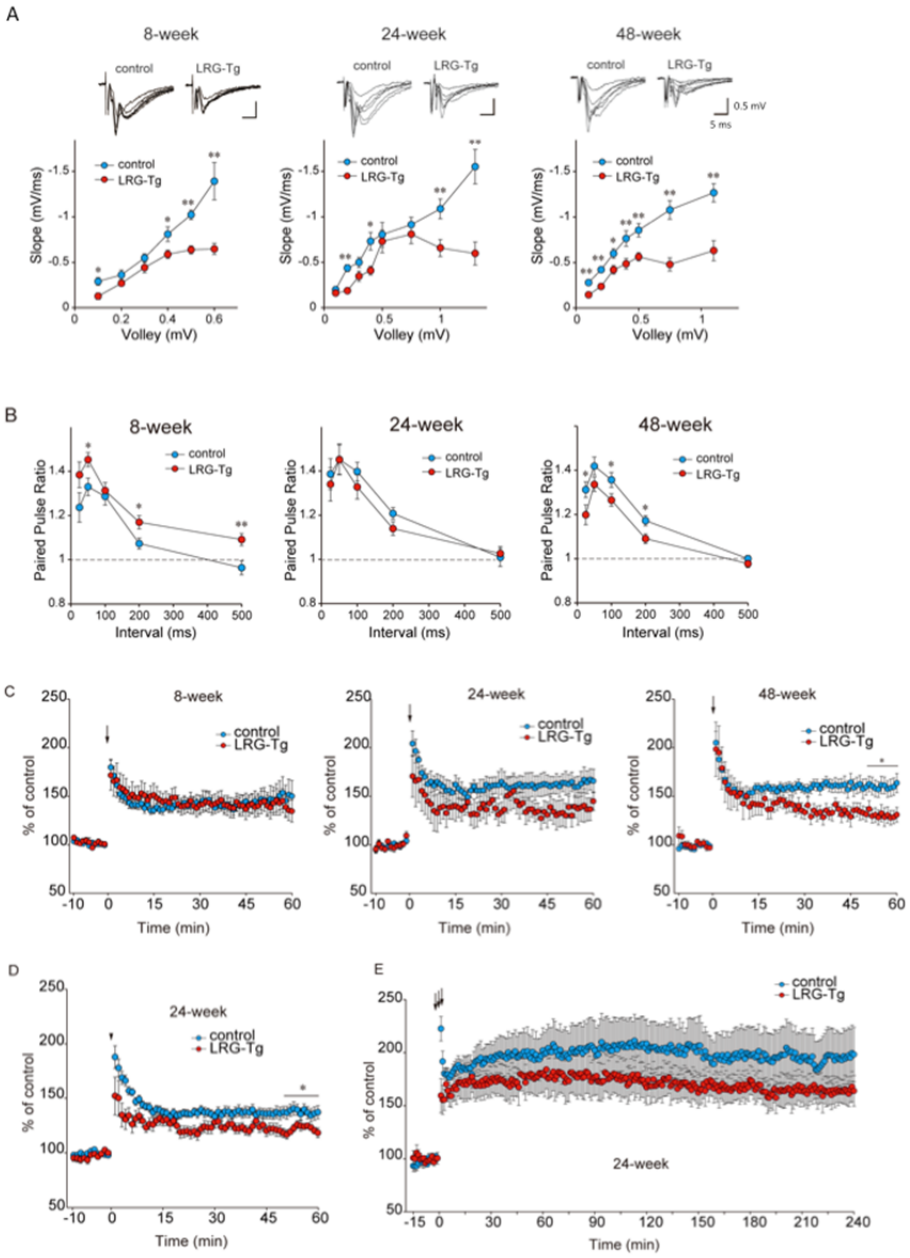

Figure 3. Electrophysiological alterations in hippocampal slices. (**A**) Evoked field excitatory post-synaptic potential (fEPSPs) slopes were averaged over four consecutive trials per min, normalized, and plotted against the fiber volley amplitude. fEPSP slopes were significantly reduced in LRG-Tg compared to control mice at all ages examined: 8-week-old control (n = 11) and LRG-Tg (n = 12),

532 24-week-old control (n = 18) and LRG-Tg (n = 18), and 48-week-old control (n = 31) and LRG-Tg (n =

533 33). (**B**) Paired-pulse ratios (PPRs, second slope/first slope) in response to paired stimuli (intervals of

534 25–500 ms) were measured following fEPSPs in the same experimental mice, and were decreased with

535 age in LRG-Tg and increased with age in control mice. (**C**) The magnitude of long-term potentiation

536 (LTP) induced by high-frequency stimulation (100 pulses at 100 Hz) was attenuated only in 48-week-old

537 LRG-Tg and was retained approximately at the same level as controls in 8- and 24-week-old LRG-Tg

538 mice: 8-week-old control (n = 11) and LRG-Tg (n = 11), 24-week-old control (n = 9) and LRG-Tg (n = 9),

539 and 48-week-old control (n = 31) and LRG-Tg (n = 33). (**D**) LTP induced with a short tetanus (30 pulses

540 at 100 Hz) was unstable in 24-week-old LRG-Tg relative to age-matched controls (n = 14 controls and 11

541 LRG-Tg). (**E**) There was, however, no difference in the magnitude of late-phase LTP induced by repeated

542 tetanus (3 trains of 100 pulses at 100 Hz) in 24-week-old control and LRG-Tg mice (n = 10 controls and

543 10 LRG-Tg).

544 Values are expressed as the mean ± S.E.M. of independent experimental groups. To assess between-group

545 differences, 2-tailed Student's *t*-tests were used.* $p < 0.05$; ** $p < 0.01$.

Figure 4

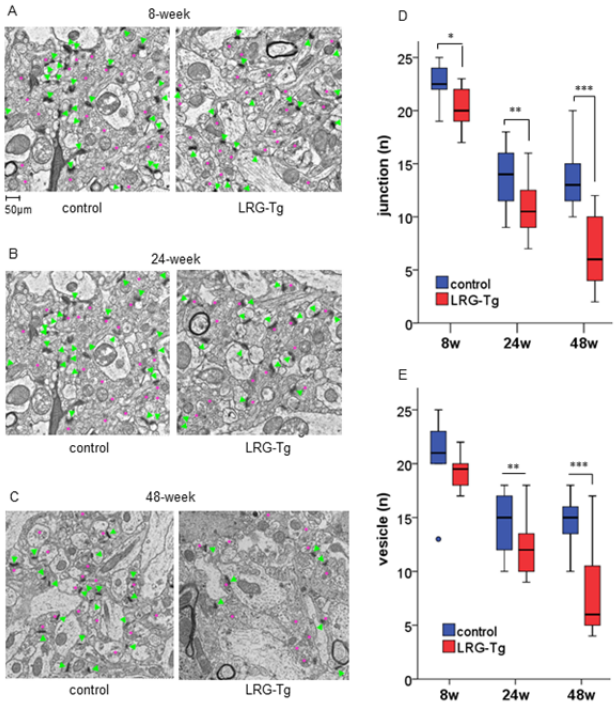

Figure 4. Electron microscopy observation of synaptic structures. (**A**) Electron microscopy (5000×) enabled the identification of synaptic vesicles (pink asterisks) and synaptic junctions (green triangles) in the CA1 hippocampal region of 8- and 24-week-old (**B**), and (**C**) 48-week-old mice. (**D**)The numbers of junctions and (**E**) vesicles counted in 10 randomly selected visual fields in the CA1 hippocampal region were significantly fewer in LRG-Tg relative to control mice, in all age groups: 8-week-old control (n = 2) and LRG-Tg (n = 2), 24-week-old control (n = 2) and LRG-Tg (n = 2), and 48-week-old control (n = 2) and LRG-Tg (n = 2).

All images displayed are representative and values are expressed as the median (interquartile range 25% and 75%) of independent experimental groups. To assess between-group differences, 2-tailed Student's *t*-tests were used. *$p < 0.05$; **$p < 0.01$; *** $p < 0.001$.

Figure 1

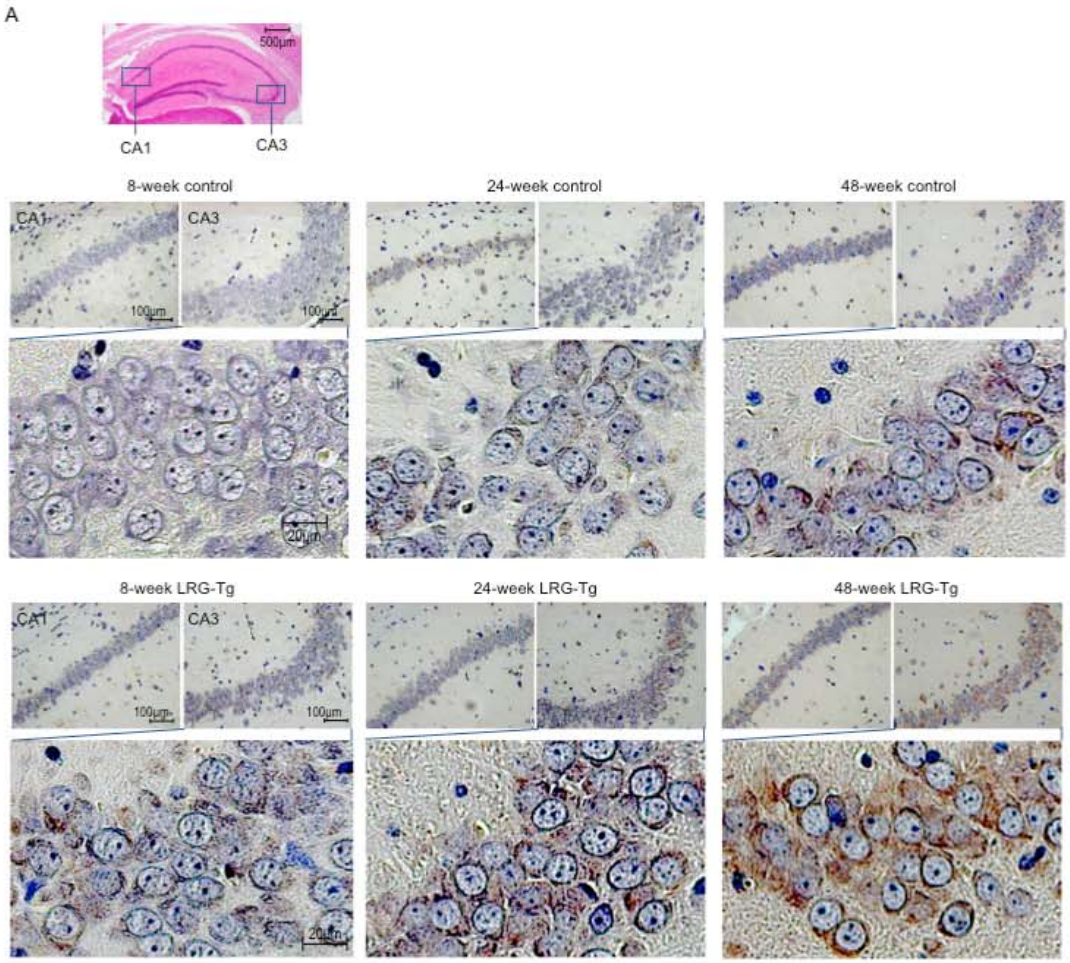
A
500μm
CA1
CA3
8-week control
24-week control
48-week control
CA1
CA3
100μm
20μm
8-week LRG-Tg
24-week LRG-Tg
48-week LRG-Tg

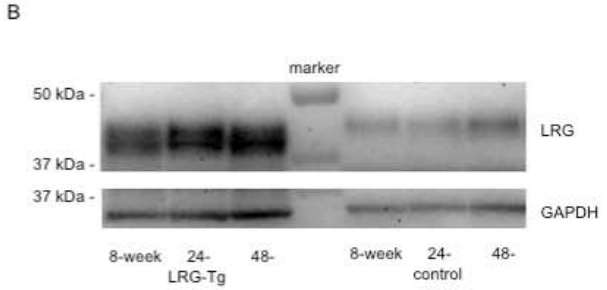
B
marker
50 kDa -
37 kDa -
37 kDa -
LRG
GAPDH
8-week
24-
48-
LRG-Tg
8-week
24-
48-
control

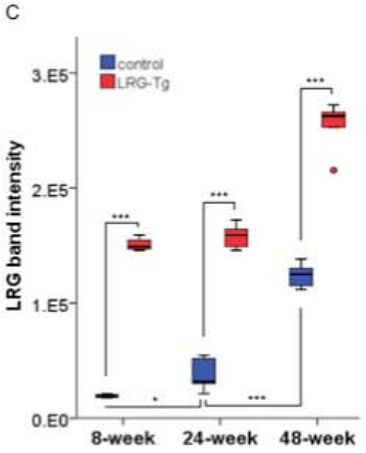
C
control
LRG-Tg
3.E5
2.E5
1.E5
0.E0
LRG band intensity
***
8-week
24-week
48-week

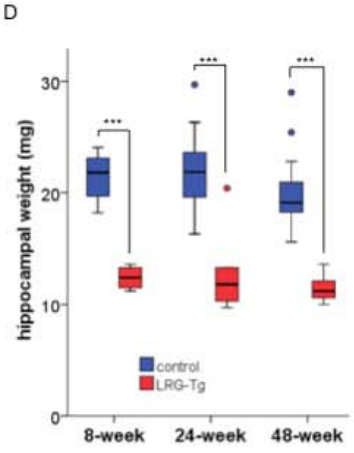
D
30
20
10
0
hippocampal weight (mg)
***
control
LRG-Tg
8-week
24-week
48-week

Figure 2

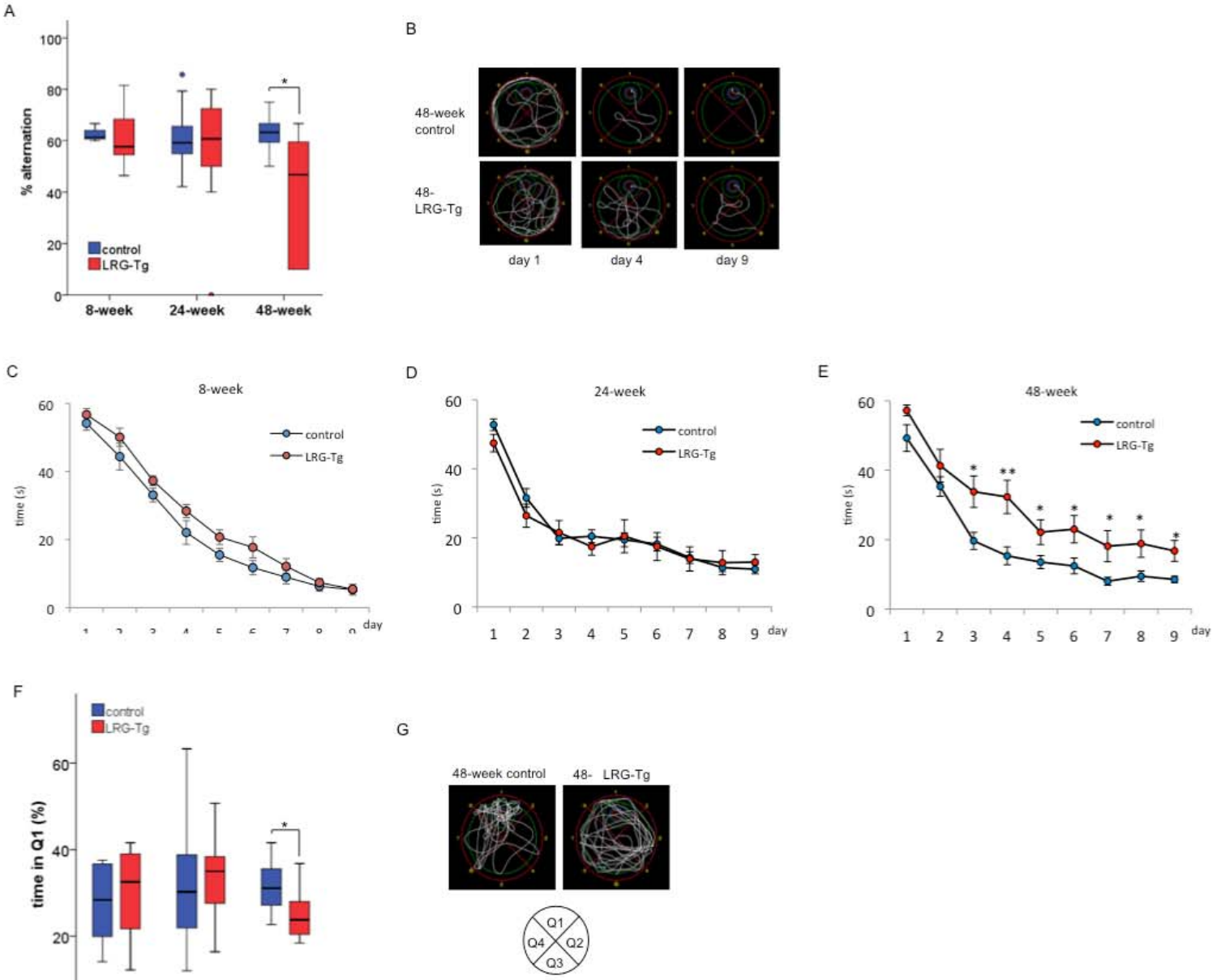
A
% alternation
control
LRG-Tg
8-week
24-week
48-week
B
48-week control
48- LRG-Tg
day 1
day 4
day 9
C
8-week
time (s)
day
D
24-week
E
48-week
F
time in Q1 (%)
G
48-week control
48- LRG-Tg
Q1
Q2
Q3
Q4

Figure 3

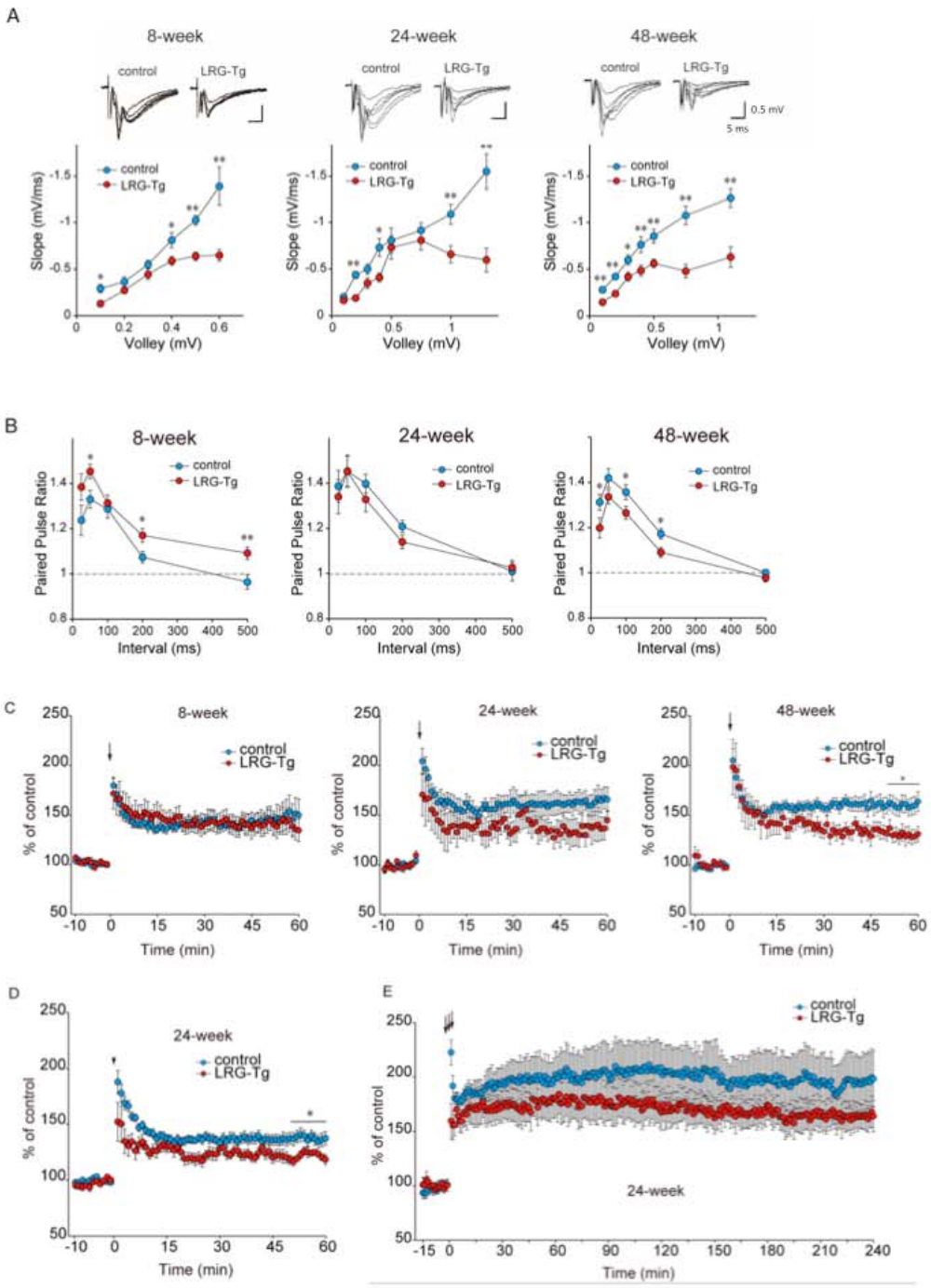
A
8-week
24-week
48-week
control
LRG-Tg
0.5 mV
5 ms
Slope (mV/ms)
Volley (mV)
B
Paired Pulse Ratio
Interval (ms)
C
% of control
Time (min)
D
E

Figure 4

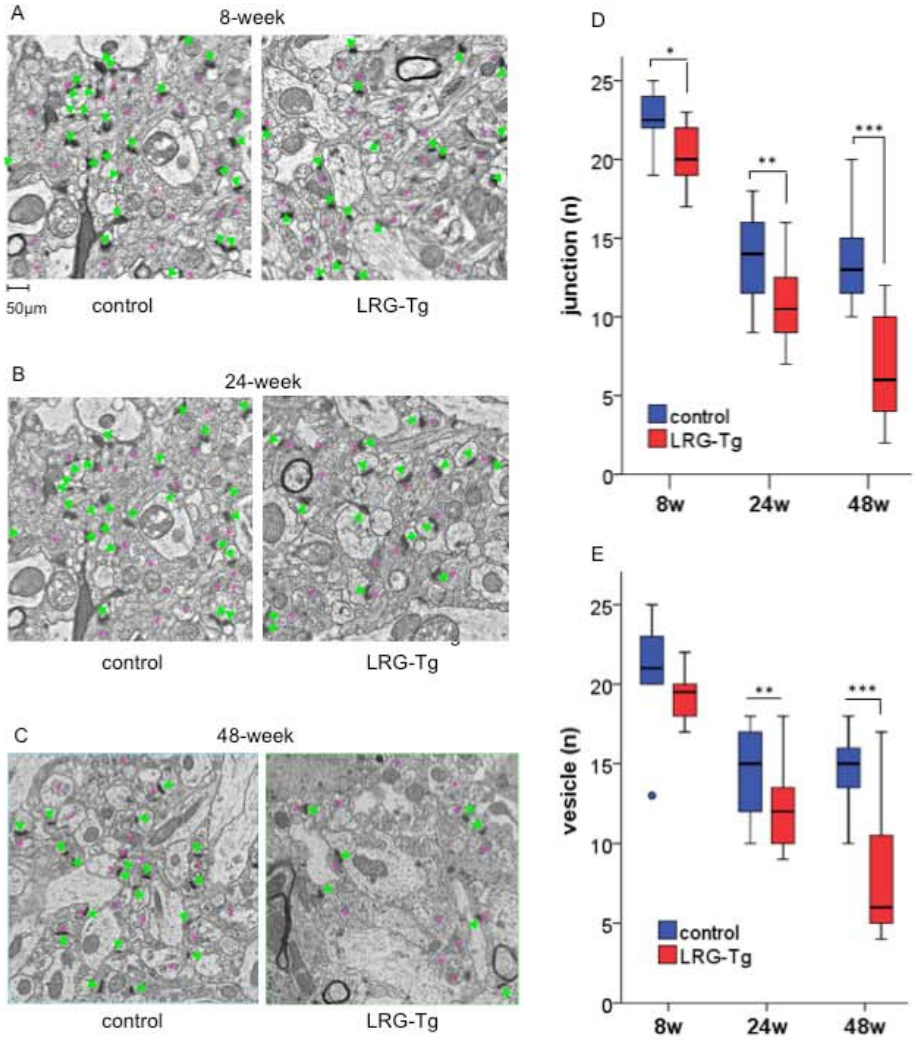
A
8-week
50μm
control
LRG-Tg
B
24-week
control
LRG-Tg
C
48-week
control
LRG-Tg
D
junction (n)
control
LRG-Tg
8w
24w
48w
E
vesicle (n)
control
LRG-Tg
8w
24w
48w

Supplementary Data 1

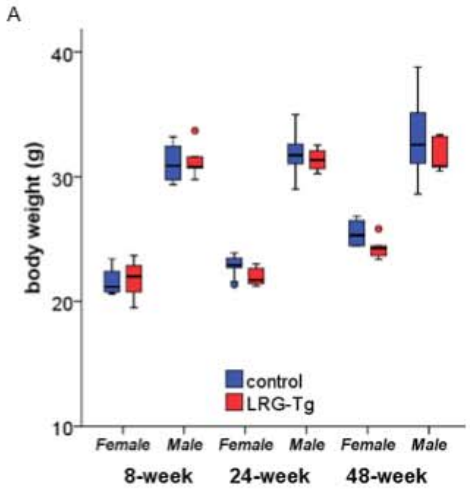

Supplementary Data 2

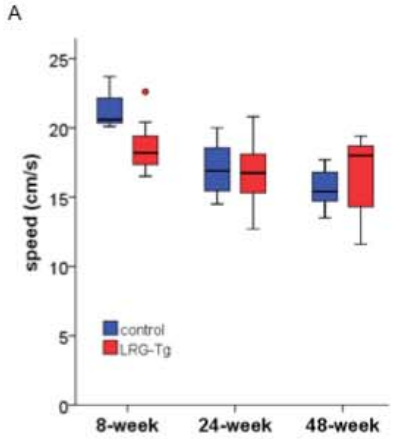

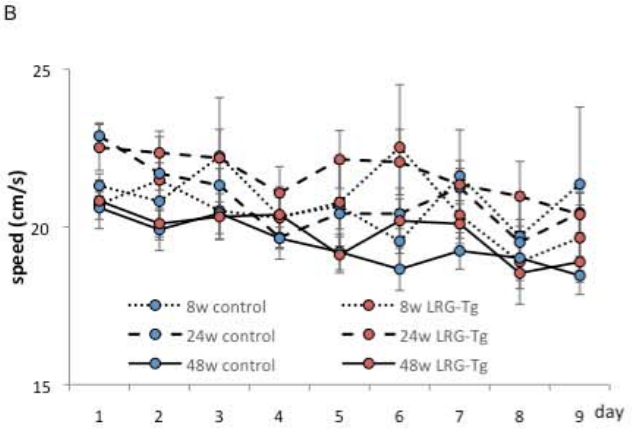

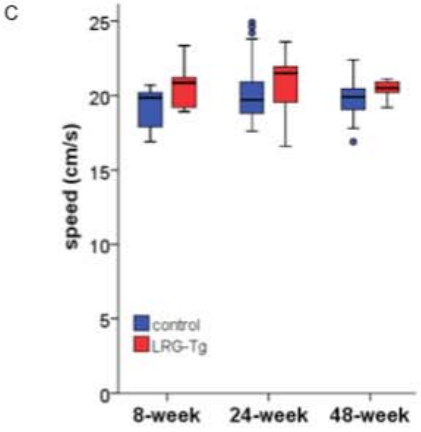

Supplementary Data 1

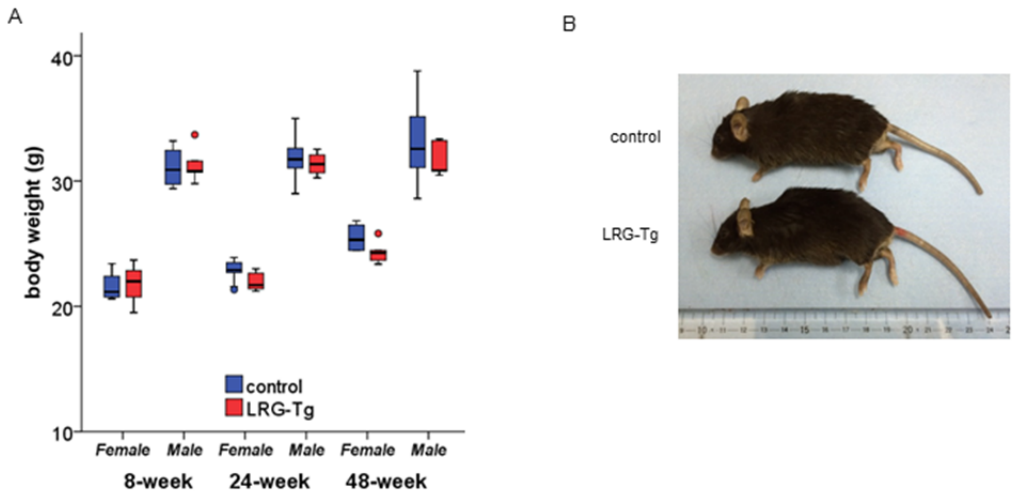

Supplementary Data 1. Gross anatomical observations in 48-week-old transgenic mice conditionally overexpressing LRG in hippocampal neurons (LRG-Tg) and control mice. (**A**) Body weight was not significantly different between groups. (**B**) No qualitative between-group differences were observed in the gross anatomy. The minimum scale indicates 1 mm.

The displayed image is representative and values are expressed as the median (~~IQR~~ interquartile range 25% and 75%) of independent experimental groups. To assess between-group differences, 2~~two~~-tailed Student's *t*-tests were used.

Supplementary Data 2

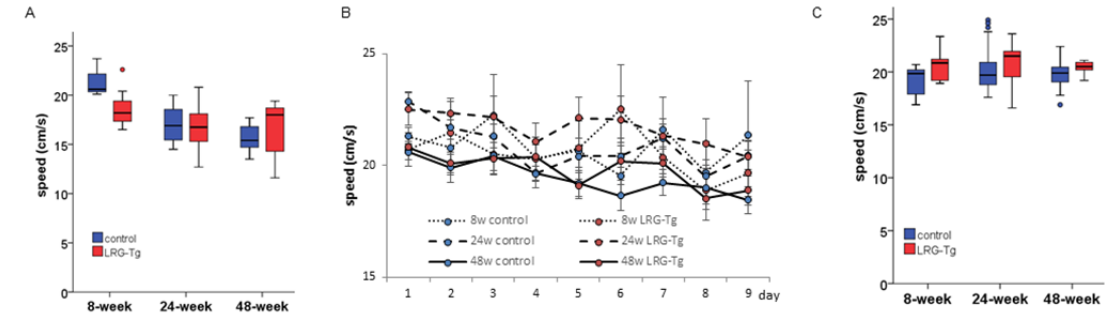

Supplementary Data 2. Walking or swimming speed recorded during the behavioral tests. (**A**) The average walking speed in the Y-maze test, which did not significantly differ between groups. (**B**) The average swimming speeds during the Morris water maze learning period and (**C**) during the probe test, which did not significantly differ between groups.

Values are expressed as the median (~~IQR~~ interquartile range 25% and 75%) for (A) and (C), the mean ± S.E.M. for (B) of independent experimental groups. To assess between-group differences, 2~~two~~-tailed Student's *t*-tests were used.

Supplementary Data 3. The complete dataset of all of the experimental results.

Refer the Excel sheet attached.

Supplementary data 3

A

		8-week control	8-week LRG-Tg	p-value	t-value	24-week control	24-week LRG-Tg	p-value	t-value	48-week control	48-week LRG-Tg	p-value	t-value
		n = 8	n = 8			n = 19	n = 14			n = 19	n = 13		
Hippocampal weight (mg)	Fig. 1D	21.4 (19.9–22.7)	12.4 (12.1–13.0)	$p < 0.001$	$t(10) = 11.187$	21.9 (19.5–23.9)	11.8 (10.3–13.3)	$p < 0.001$	$t(10) = 6.948$	19.1 (18.2–21.4)	11.2 (10.3–12.4)	$p < 0.001$	$t(23) = 8.981$

B

			8-week control	8-week LRG-Tg	p-value	t-value	24-week control	24-week LRG-Tg	p-value	t-value	48-week control	48-week LRG-Tg	p-value	t-value
Y-maze			n = 6	n = 11			n = 47	n = 18			n = 17	n = 9		
% alternation	Fig. 2A		62.7 (61.4–66.7)	61.4 (54.4–70.7)	$p = 0.744$	$t(11) = 0.335$	59.1 (54.7–65.6)	60.8 (48.5–72.6)	$p = 0.329$	$t(19) = 0.816$	63.3 (59.2–67.6)	46.7 (10.0–59.5)	$p = 0.017$	$t(9) = 2.938$
speed (cm/s)	Supp. 2A		20.5 (20.1–22.7)	17.4 (15.3–19.4)	$p = 0.104$	$t(6) = 2.310$	16.9 (15.4–18.6)	16.8 (15.5–18.2)	$p = 0.399$	$t(25) = 0.996$	15.4 (14.7–16.9)	18.0 (14.5–19.0)	$p = 0.312$	$t(8) = 1.078$
Morris water maze, learning			n = 6	n = 6			n = 36	n = 16			n = 13	n = 9		
time (s)	Fig. 2C,D,E	day 1	54.2 ± 2.0	56.7 ± 1.8	$p = 0.370$	$t(10) = 0.940$	52.8 ± 1.7	47.4 ± 2.5	$p = 0.090$	$t(29) = 1.753$	49.3 ± 3.9	57.2 ± 1.5	$p = 0.066$	$t(27) = 1.916$
		day 2	44.4 ± 3.9	50.1 ± 2.6	$p = 0.259$	$t(9) = 1.200$	31.6 ± 2.7	26.4 ± 3.4	$p = 0.240$	$t(36) = 1.194$	35.3 ± 2.8	41.3 ± 4.7	$p = 0.287$	$t(21) = 1.092$
		day 3	33.1 ± 2.0	37.3 ± 1.5	$p = 0.125$	$t(9) = 1.692$	19.8 ± 1.9	21.5 ± 3.5	$p = 0.671$	$t(25) = 0.430$	19.6 ± 2.5	33.8 ± 4.5	$p = 0.013$	$t(19) = 2.740$
		day 4	22.1 ± 3.5	28. ± 1.9	$p = 0.151$	$t(8) = 1.590$	20.5 ± 1.9	17.5 ± 2.5	$p = 0.341$	$t(34) = 0.965$	15.3 ± 2.6	32.3 ± 4.8	$p = 0.006$	$t(19) = 3.113$
		day 5	15.5 ± 1.9	20.7 ± 2.1	$p = 0.101$	$t(10) = 1.805$	19.4 ± 2.0	20.5 ± 4.8	$p = 0.842$	$t(21) = 0.202$	13.5 ± 1.9	22.1 ± 3.6	$p = 0.045$	$t(19) = 2.141$
		day 6	11.7 ± 2.1	17.7 ± 3.1	$p = 0.143$	$t(9) = 1.605$	18.2 ± 2.0	17.5 ± 4.0	$p = 0.877$	$t(23) = 0.157$	12.4 ± 2.3	23.0 ± 3.9	$p = 0.031$	$t(20) = 2.327$
		day 7	9 ± 2.0	12.1 ± 2.3	$p = 0.317$	$t(10) = 1.053$	14.3 ± 1.7	13.9 ± 3.5	$p = 0.924$	$t(22) = 0.100$	8.0 ± 1.2	18.1 ± 4.5	$p = 0.046$	$t(14) = 2.193$
		day 8	6.3 ± 1.4	7.4 ± 1.2	$p = 0.558$	$t(10) = 0.607$	11.4 ± 1.2	12.8 ± 3.5	$p = 0.708$	$t(18) = 0.380$	9.5 ± 1.5	18.9 ± 4.0	$p = 0.041$	$t(16) = 2.218$
		day 9	5.3 ± 1.6	5.4 ± 0.8	$p = 0.932$	$t(7) = 0.088$	10.9 ± 1.3	13.0 ± 2.2	$p = 0.433$	$t(27) = 0.797$	8.5 ± 0.9	16.7 ± 3.0	$p = 0.020$	$t(14) = 2.612$
speed (cm/s)	Supp. 2B	day 1	21.3 ± 0.4	20.7 ± 0.8	$p = 0.515$	$t(7) = 0.685$	22.9 ± 0.4	22.8 ± 0.8	$p = 0.955$	$t(23) = 0.057$	20.6 ± 0.4	20.8 ± 0.3	$p = 0.642$	$t(25) = 0.470$
		day 2	20.8 ± 1.2	21.5 ± 1.4	$p = 0.722$	$t(10) = 0.365$	21.7 ± 0.5	22.5 ± 0.6	$p = 0.367$	$t(33) = 0.914$	19.9 ± 0.7	20.1 ± 0.4	$p = 0.812$	$t(24) = 0.241$
		day 3	22.2 ± 1.9	20.5 ± 0.7	$p = 0.420$	$t(6) = 0.866$	21.3 ± 0.5	22.4 ± 0.9	$p = 0.284$	$t(24) = 1.096$	20.4 ± 0.8	20.3 ± 0.7	$p = 0.920$	$t(25) = 0.101$
		day 4	20.3 ± 0.6	20.3 ± 1.0	$p = 0.963$	$t(8) = 0.477$	19.7 ± 0.3	21.5 ± 0.9	$p = 0.068$	$t(18) = 1.942$	19.6 ± 0.7	20.4 ± 0.7	$p = 0.427$	$t(24) = 0.807$
		day 5	20.7 ± 1.0	20.8 ± 1.4	$p = 0.951$	$t(10) = 0.063$	20.4 ± 0.5	22.4 ± 0.9	$p = 0.064$	$t(23) = 1.949$	19.2 ± 0.6	19.1 ± 0.6	$p = 0.911$	$t(24) = 0.112$
		day 6	19.5 ± 0.8	22.5 ± 2.0	$p = 0.209$	$t(7) = 1.383$	20.4 ± 0.5	22.5 ± 1.0	$p = 0.090$	$t(20) = 1.779$	18.7 ± 0.7	20.2 ± 1.0	$p = 0.228$	$t(18) = 1.247$
		day 7	21.6 ± 1.5	20.4 ± 0.7	$p = 0.472$	$t(7) = 0.761$	21.2 ± 0.9	22.2 ± 1.0	$p = 0.471$	$t(35) = 0.730$	19.2 ± 0.6	20.1 ± 0.6	$p = 0.326$	$t(23) = 1.004$
		day 8	11.7 ± 0.7	18.9 ± 1.3	$p = 0.686$	$t(10) = 0.416$	19.5 ± 0.5	21.3 ± 1.1	$p = 0.151$	$t(21) = 1.492$	19.0 ± 0.5	18.5 ± 0.5	$p = 0.518$	$t(25) = 0.656$
		day 9	21.4 ± 1.4	19.7 ± 1.0	$p = 0.542$	$t(7) = 0.642$	20.4 ± 0.6	20.6 ± 0.7	$p = 0.891$	$t(35) = 0.138$	18.5 ± 0.6	18.9 ± 0.6	$p = 0.628$	$t(23) = 0.491$
Morris water maze, probe			n = 6	n = 6			n = 38	n = 22			n = 19	n = 9		
time in Q1 (%)	Fig. 2F		27.5 (20.8–37.4)	29.9 (22.2–39.0)	$p = 0.691$	$t(10) = 0.409$	30.3 (23.4–39.5)	35.0 (29.7–39.1)	$p = 0.434$	$t(38) = 0.788$	31.1 (28.7–37.2)	23.7 (22.5–29.2)	$p = 0.046$	$t(14) = 2.187$
speed (cm/s)	Supp. 2C		19.2 (17.8–20.3)	20.7 (19.7–22.3)	$p = 0.318$	$t(9) = 1.058$	19.7 (18.8–21.0)	22.0 (19.5–22.5)	$p = 0.395$	$t(24) = 0.867$	19.9 (19.0–20.7)	20.5 (20.2–21.0)	$p = 0.238$	$t(19) = 1.219$

C

			8-week control	8-week LRG-Tg	p-value	t-value	24-week control	24-week LRG-Tg	p-value	t-value	48-week control	48-week LRG-Tg	p-value	t-value
			n = 11	n = 12			n = 18	n = 18			n = 31	n = 33		
Slope (mV/ms)	Fig. 3A	0.1 mV	−0.29 ± 0.04	−0.13 ± 0.04	$p = 0.017$	$t(21) = 2.590$	−0.20 ± 0.02	−0.16 ± 0.02	$p = 0.167$	$t(34) = 1.414$	−0.28 ± 0.02	−0.15 ± 0.01	$p < 0.001$	$t(62) = 5.513$
		0.2 mV	−0.36 ± 0.05	−0.27 ± 0.03	$p = 0.131$	$t(21) = 1.574$	−0.44 ± 0.04	−0.19 ± 0.02	$p < 0.001$	$t(34) = 5.590$	−0.42 ± 0.03	−0.24 ± 0.02	$p < 0.001$	$t(62) = 4.627$
		0.4 mV	−0.81 ± 0.08	−0.59 ± 0.05	$p = 0.028$	$t(21) = 2.354$	−0.72 ± 0.10	−0.42 ± 0.05	$p = 0.011$	$t(34) = 2.683$	−0.76 ± 0.09	−0.49 ± 0.06	$p = 0.009$	$t(62) = 2.712$
		0.5 mV	−1.02 ± 0.05	−0.64 ± 0.04	$p < 0.001$	$t(21) = 5.983$	−0.80 ± 0.13	−0.72 ± 0.14	$p = 0.716$	$t(34) = 0.366$	−0.86 ± 0.07	−0.56 ± 0.05	$p = 0.001$	$t(62) = 3.412$
		0.6 mV	−1.39 ± 0.20	−0.65 ± 0.06	$p < 0.001$	$t(21) = 5.983$								
		0.75 mV					−0.91 ± 0.08	−0.81 ± 0.10	$p = 0.440$	$t(34) = 0.781$	−1.08 ± 0.10	−0.48 ± 0.07	$p < 0.001$	$t(62) = 4.846$
		1.0 mV					−1.09 ± 0.11	−0.66 ± 0.09	$p = 0.005$	$t(34) = 3.025$				
		1.1 mV									−1.27 ± 0.10	−0.63 ± 0.11	$p < 0.001$	$t(62) = 4.252$
		1.3 mV					−1.55 ± 0.19	−0.60 ± 0.13	$p < 0.001$	$t(34) = 4.127$				
PPR	Fig. 3B	25 ms	1.24 ± 0.06	1.38 ± 0.07	$p = 0.115$		1.39 ± 0.08	1.34 ± 0.07	$p = 0.654$		1.32 ± 0.04	1.20 ± 0.04	$p = 0.040$	
		50 ms	1.33 ± 0.03	1.46 ± 0.04	$p = 0.026$		1.45 ± 0.07	1.45 ± 0.07	$p = 0.989$		1.42 ± 0.03	1.34 ± 0.04	$p = 0.120$	
		100 ms	1.29 ± 0.04	1.31 ± 0.04	$p = 0.621$		1.40 ± 0.05	1.33 ± 0.04	$p = 0.319$		1.36 ± 0.03	1.27 ± 0.03	$p = 0.038$	
		200 ms	1.07 ± 0.03	1.17 ± 0.03	$p = 0.023$		1.21 ± 0.03	1.14 ± 0.03	$p = 0.105$		1.17 ± 0.02	1.09 ± 0.02	$p = 0.012$	
		500 ms	0.96 ± 0.03	1.09 ± 0.03	$p = 0.006$		1.01 ± 0.03	1.03 ± 0.04	$p = 0.731$		1.00 ± 0.02	0.98 ± 0.01	$p = 0.344$	
LTP (%)	Fig. 3C	HFS*	n = 11	n = 11			n = 9	n = 9			n = 12	n = 14		
			147.4 ± 14.5	140.3 ± 11.0	$p = 0.698$	$t(20) = 0.393$	162.7 ± 11.2	136.3 ± 12.2	$p = 0.130$	$t(16) = 1.595$	160 ± 8.5	130.4 ± 7.3	$p = 0.014$	$t(24) = 2.6573$
	Fig. 3D	STS**					n = 14	n = 11						
							135.5 ± 5.1	122.9 ± 2.1	$p = 0.047$	$t(23) = 2.309$				
	Fig. 3E	3 trains of HFS					n = 10	n = 10						
							193.6 ± 25.6	164.1 ± 13.1	$p = 0.324$	$t(18) = 1.025$				

*HFS: high-frequency stimulation **STS: short tetanus stimulation

D

		8-week control	8-week LRG-Tg	p-value	t-value	24-week control	24-week LRG-Tg	p-value	t-value	48-week control	48-week LRG-Tg	p-value	t-value
		n = 4	n = 4			n = 5	n = 7			n = 7	n = 5		
LRG	Fig. 1C	23486 (20985–24068)	158342 (150670–160354)	$p < 0.001$	$t(3) = 43.699$	31939 (25775–53374)	159132 (157685–16324)	$p < 0.001$	$t(7) = 2.615$	125131 (110130–134895)	272569 (255402–286752)	$p < 0.001$	$t(6) = 11.051$
						＊8-week control vs 24- control		$p = 0.047$	$t(4) = 2.840$	＊24-week control vs 48- control		$p < 0.001$	$t(6) = 7.362$

E

		8-week control n = 2	8-week LRG-Tg n = 2	p-value	t-value	24-week control n = 2	24-week LRG-Tg n = 2	p-value	t-value	48-week control n = 2	48-week LRG-Tg n = 2	p-value	t-value
junction (n)	Fig. 4D	22.6 (22.4–23.9)	20.1(18.9–22.8)	$p = 0.026$	$t(18) = 2.420$	14.0 (12.3–16.8)	10.5 (8.8–12.8)	$p = 0.002$	$t(34) = 3.319$	12.5 (12.1–15.0)	6.0 (3.8–10.3)	$p < 0.001$	$t(36) = 7.090$
vesicles (n)	Fig. 4E	20.9 (20.0–23.6)	19.5 (17.8–21.2)	$p = 0.250$	$t(13) = 1.205$	15.0 (12.4–17.6)	12.0 (10.0–13.1)	$p = 0.005$	$t(34) = 2.971$	15.0 (13.8–16.7)	6.0 (5.1–10.4)	$p < 0.001$	$t(26) = 5.835$

F

		8-week Female				24-week Female				48-week Female			
		control (n = 4)	LRG-Tg (n = 3)	p-value	t-value	control (n = 10)	LRG-Tg (n = 7)	p-value	t-value	control (n = 4)	LRG-Tg (n = 5)		
Body weight (g)	Supp. 1A	21.6 (20.8–22.0)	22.7 (20.9–22.6)	$p = 0.915$	$t(3) = 0.115$	22.9 (22.4–23.5)	21.7 (21.2–22.9)	p = 0.055	$t(13) = 1.964$	25.3 (24.5–26.5)	24.3 (23.5–24.5)	$p = 0.164$	$t(6) = 1.587$
		8-week Male				24-week Male				48-week Male			
		control (n = 4)	LRG-Tg (n = 5)	p-value	t-value	control (n = 15)	LRG-Tg (n = 4)	p-value	t-value	control (n = 12)	LRG-Tg (n = 5)		
		31.1 (29.9–33.6)	31.3 (30.9–32.3)	$p = 0.845$	$t(6) = 0.205$	31.7 (30.8–32.7)	31.4 (30.5–32.3)	$p = 0.532$	$t(6) = 0.997$	32.6 (31.0–35.7)	30.8 (30.6–35.3)	$p = 0.242$	$t(15) = 1.219$